

Odd-Order Aberration-Cancellation in Correlated-Photon Imaging

D.S. Simon^{1,2} and A.V. Sergienko^{1,2,3}

¹*Dept. of Electrical and Computer Engineering,*

Boston University, 8 Saint Mary's St., Boston, MA 02215

²*Photonics Center, Boston University, 8 Saint Mary's St., Boston, MA 02215*

³*Dept. of Physics, Boston University, 590 Commonwealth Ave., Boston, MA 02215*

We discuss a correlated two-photon imaging apparatus that is capable of producing images that are free of the effects of odd-order aberration introduced by the optical system. We show that both quantum-entangled and classically correlated light sources are capable of producing the desired spatial-aberration cancellation.

PACS numbers: 42.30.Va, 42.15.Fr, 42.50.-p

I. INTRODUCTION

Two-photon imaging, also known as ghost imaging, involves the use of coincidence measurements to form images via photons that never interacted with the object being viewed. It has been a topic of great interest since its discovery using entangled photon pairs [1]. Initially, it was believed that the entanglement was a necessary ingredient for the effect, but it has since been found that most aspects of ghost imaging can be simulated using spatially-correlated classical light [2, 3], including thermal and speckle sources [4–9].

Separately, it has been demonstrated that the entangled photon pairs produced in spontaneous parametric downconversion (SPDC) may also be used to cancel some of the effects of frequency dispersion [10–12] or spatial dispersion (aberration) [13–15] in interferometer experiments.

The goal here is to show that two-photon imaging can be done with spatially correlated pairs of light beams in such a way that odd-order aberration effects introduced by an imaging system may be cancelled. This may be done with either classically correlated beams or quantum entangled photon pairs. The key idea is to partially collapse the two arms of the ghost-imaging setup so that *both* of the output beams pass through the *same* optical system in an anticorrelated manner, but with only one of the beams passing through the object. Here we will illustrate the method using the simplest possible imaging system, a single lens.

The outline of the paper is as follows. In section II, we review the basic idea of correlated two-photon imaging. In section III we discuss aberration-cancelled two-photon imaging with an entangled light source. In section IV we briefly discuss how to do the same with a classical source, followed by conclusions in section V.

II. TWO-PHOTON GHOST IMAGING

Two-photon correlated imaging, or ghost imaging [1], is done with an apparatus like the one depicted schematically in figure 1. In the original version, the correlated

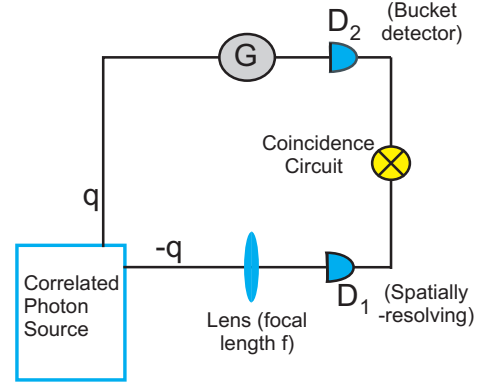


FIG. 1: (Color online) Schematic depiction of two-photon (ghost) imaging setup used to view object G .

photon source is a $\chi^{(2)}$ nonlinear crystal pumped by a laser, leading to spontaneous parametric downconversion. This is the source we will use in section III. Entangled photon pairs with anticorrelated transverse spatial momenta \mathbf{q} and $-\mathbf{q}$ travel along the two arms of the apparatus. The object to be viewed introduces a modulation (either the transmittance or reflectance of the object), given by a function $G(\mathbf{x})$. This object is placed in arm 2 (the upper branch), followed by a large bucket detector, D_2 . The detector's area is integrated over, so D_2 can not record any information on the position or momentum of the photon that reached the object; all this detector is able to tell us is whether the photon reached the detector unimpeded, or whether its passage was blocked by the object. In the other branch of the apparatus there is no object, and all of the photons reach an array of pointlike detectors or some other form of spatially resolving detector without hindrance. A coincidence circuit is used to record a count every time a photon detection occurs simultaneously (within the coincidence time window) at both detectors. By plotting the coincidence rate as a function of position x_1 in detector 1, we build up an image of the object. This is true even though photons that actually encountered the object in branch 2 left no record of the object's position, and the photons in branch 1 that do carry position information never encounter the object.

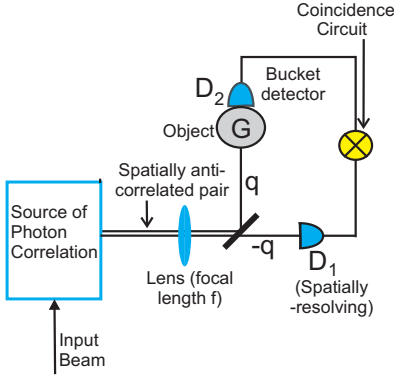


FIG. 2: (Color online) Schematic depiction of setup for odd-order aberration-cancelled imaging of object G .

The essential ingredient is the spatial correlation of the downconverted photon pair. The question arose as to whether the entanglement of the photons was necessary, or if a classical source with anticorrelated transverse momenta could mimic the effect. It was found [2, 3] that this was indeed possible. The correlated light source in this case consists of a beam steering modulator (a rotating mirror, for example) which directs a classical light beam through a range of \mathbf{q} vectors, illuminating different spots on the object. The beamsplitter then turns the single beam of transverse momentum \mathbf{q} into a pair of beams with momenta \mathbf{q} and $-\mathbf{q}$. The results were similar to those with the entangled source, but with half the visibility. It has since been shown that spatial correlations present in radiation produced using thermal and speckle sources may also lead to ghost imaging ([4–9]).

III. ODD-ORDER ABERRATION CANCELLATION IN TWO-PHOTON IMAGING

Many optical devices work by adding position-dependent phase shifts to a beam as it passes through the device. A lens, for example, produces focusing by adding to the beam a quadratic phase shift $e^{-\frac{ik}{2f}\mathbf{x}^2}$, where k , f and \mathbf{x} are the wavenumber of the beam, the focal length of the lens, and the displacement of the given point in the beam from the axis of the lens. However, imperfections in the shape of the lens and variations in the index of refraction of the material from which it is made may lead to additional unwanted phase shifts $e^{i\phi(\mathbf{x})}$ beyond those intended. These unwanted phases are an example of optical aberration: they lead to distortions of the outgoing wavefronts, and consequently produce distortion in the final image. The aberration function $\phi(\mathbf{x})$ may be parameterized in a number of ways, for example by expanding in Zernike or Seidel polynomials [16–18]. Here we are uninterested in the details of how the function is represented and are concerned only with the fact that it may be split into a sum of parts which are either even or

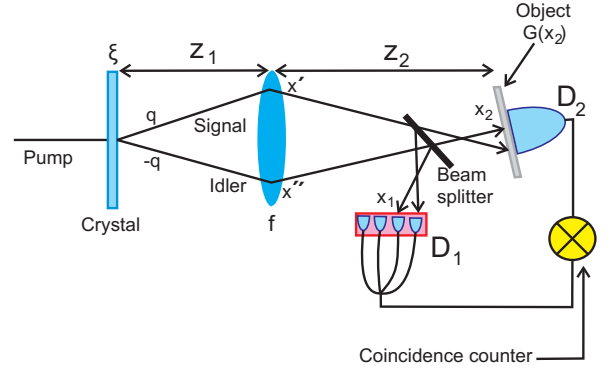


FIG. 3: (Color online) Implementation of scheme of fig. 2 using parametric downconversion.

odd under reflection about the axis:

$$\phi(\mathbf{x}) = \phi_{\text{even}}(\mathbf{x}) + \phi_{\text{odd}}(\mathbf{x}), \quad (1)$$

where

$$\phi_{\text{even}}(-\mathbf{x}) = \phi_{\text{even}}(\mathbf{x}), \quad (2)$$

$$\phi_{\text{odd}}(-\mathbf{x}) = -\phi_{\text{odd}}(\mathbf{x}). \quad (3)$$

The even-order terms include astigmatism and spherical aberration, while coma contributes to the odd-order terms.

We now wish to take the two-photon imaging setup of fig. 1 and alter it in order to cancel as much of the aberration of the lens as possible. Note that we should aim only to cancel the odd part of the aberration, since cancellation of the even-order phases would also completely cancel the effect (the quadratic phase shift) of the lens itself.

So consider the setup shown in fig. 2. This is similar to fig. 1, but with one main difference: we have partially merged the two arms, separating the photons in each pair only *after* they have passed through the lens. The two photons both arise from the same well-localized point ξ in the source, but emerge with opposite transverse momenta $\pm\mathbf{q}$. So *both* pass through the same lens, but tend to pass through it on opposite sides of the axis.

Fig. 3 shows a slightly more detailed picture of a particular embodiment of this scheme, using entangled photon pairs produced via parametric downconversion. Suppose the field in the pump beam as it enters the crystal is $E_p(\xi)$. We arrange for the distances to satisfy the imaging condition

$$\frac{1}{z_1} + \frac{1}{z_2} = \frac{1}{f}. \quad (4)$$

The lens will have a pupil function which we assume to consist of the usual quadratic phase plus an additional phase function describing aberrations:

$$p(\mathbf{x}) = e^{-i(\mathbf{x}^2/2f)} e^{i\phi(\mathbf{x})}. \quad (5)$$

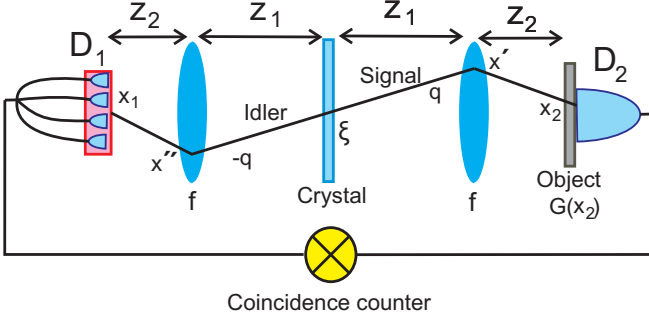


FIG. 4: (Color online) Unfolded version of the apparatus in fig. 3, with the signal and idler drawn as a single continuous ray.

The beam splitter sends half of the photons to a spatially-resolving detector D_1 , the other half to a large bucket detector D_2 , with no spatial resolution. The object introduces a modulation $G(\mathbf{x}_2)$ only in branch 2. The impulse response function for beam j ($j = 1, 2$) to travel from transverse position ξ in the crystal plane to transverse position \mathbf{x}_j in the detection plane is then

$$h(\xi, \mathbf{x}_j) = H_j(\mathbf{x}_j) e^{ik[(\xi^2/z_1) + (\mathbf{x}_j/z_2)]/2} \times \int e^{-ik[(\xi/z_1) + (\mathbf{x}_j/z_2)] \cdot \mathbf{x}'} e^{i\phi(\mathbf{x}')} d^2x', \quad (6)$$

where

$$H_j(\mathbf{x}_j) = \begin{cases} 1, & \text{for } j = 1 \\ G(\mathbf{x}_2), & \text{for } j = 2. \end{cases} \quad (7)$$

One further view of the apparatus is useful. Fig. 4 shows an unfolded version of the setup in the Klyshko picture [19, 20]. In this picture, the signal and idler can be viewed as a single continuous ray from one detector to the other. In the approximation of a plane wave pump, this ray is undeflected at the crystal because of the perfect anti-correlation between the signal and the idler wave vector directions ($\mathbf{q} = -\mathbf{q}$), causing the signal and idler to hit the lens at a pair of points arranged symmetrically about the point where the ray crosses the crystal, $\mathbf{x}' - \xi = \xi - \mathbf{x}''$.

Assuming a thin crystal and narrow-band filters in the beams, the coincidence amplitude (or equivalently, the two-photon wavefunction) in the detection plane can be written (up to overall normalization) in the simple form [21]

$$\psi(\mathbf{x}_1, \mathbf{x}_2) = \int E_p(\xi) h_1(\xi, \mathbf{x}_1) h_2(\xi, \mathbf{x}_2) d^2\xi \quad (8)$$

$$= \int E_p(\xi) G(\mathbf{x}_2) e^{(ik\xi^2/z_1)} e^{(ik/2z_2)(x_1^2 + x_2^2)} \times e^{-ik\xi \cdot (\mathbf{x}' + \mathbf{x}'')/z_1} e^{-ik(\mathbf{x}_1 \cdot \mathbf{x}' + \mathbf{x}_2 \cdot \mathbf{x}'')} \times e^{i(\phi(\mathbf{x}') + \phi(\mathbf{x}''))} d^2\xi d^2x' d^2x''. \quad (9)$$

The coincidence rate is

$$R(x_1) = \int d^2x_2 |\psi(\mathbf{x}_1, \mathbf{x}_2)|^2 \quad (10)$$

If we define

$$F(\xi) = E_p(\xi) e^{ik\xi^2/z_1}, \quad (11)$$

then the amplitude may be written in the form

$$\psi(\mathbf{x}_1, \mathbf{x}_2) = G(\mathbf{x}_2) e^{ik(\mathbf{x}_2^2 + \mathbf{x}_1^2)/2z_2} \times \int \tilde{F}\left(\frac{k(\mathbf{x}' + \mathbf{x}'')}{z_1}\right) e^{-ik(\mathbf{x}_1 \cdot \mathbf{x}' + \mathbf{x}_2 \cdot \mathbf{x}'')/z_2} \times e^{i(\phi(\mathbf{x}') + \phi(\mathbf{x}''))} d^2x' d^2x'' d^2\xi.$$

For simplicity, we take the pump to be an approximate plane wave over the extent of the object, so that we may set $E_p(\xi)$ equal to a constant. We also assume that we are working in the far field, where the ξ^2 term in the exponential may be neglected in comparison with the other terms. In that case, we find $\tilde{F}\left(\frac{k}{z_1}(\mathbf{x}' + \mathbf{x}'')\right)$ is proportional to $\delta^{(2)}(\mathbf{x}' + \mathbf{x}'')$, so that the amplitude reduces to

$$\psi(\mathbf{x}_1, \mathbf{x}_2) = G(\mathbf{x}_2) e^{ik(\mathbf{x}_2^2 + \mathbf{x}_1^2)/(2z_2)} \quad (13)$$

$$\times \int e^{-ik(\mathbf{x}_1 - \mathbf{x}_2) \cdot \mathbf{x}'/z_2} e^{2i\phi_{\text{even}}(\mathbf{x}')} d^2x' = G(\mathbf{x}_2) e^{ik(\mathbf{x}_2^2 + \mathbf{x}_1^2)/(2z_2)} \times \tilde{\Phi}_{\text{even}}\left(\frac{k(\mathbf{x}_1 - \mathbf{x}_2)}{z_2}\right), \quad (14)$$

where we have defined

$$\Phi_{\text{even}}(x) = e^{2i\phi_{\text{even}}(\mathbf{x})}, \quad (15)$$

and the tilde denotes the Fourier transform. Given this, the coincidence rate is then

$$R(\mathbf{x}_1) = \int d^2x_2 |\psi(\mathbf{x}_1, \mathbf{x}_2)|^2 \quad (16)$$

$$= \int d^2x_2 \left| G(\mathbf{x}_2) \tilde{\Phi}_{\text{even}}\left(\frac{k}{z_2}(\mathbf{x}_1 - \mathbf{x}_2)\right) \right|^2 \quad (17)$$

Eq. 17 is our main result. Note that it depends only on the even-order aberrations; all odd-order terms have dropped out. In the special case that there is no aberration in the lens, this reduces to

$$R(\mathbf{x}_1) = |G(\mathbf{x}_1)|^2. \quad (18)$$

It is apparent that we will always obtain unit magnification.

The odd-order aberration cancellation is exact only in the far field and in the case of a plane wave pump. As the distances involved decrease or as the pump amplitude deviates from a constant, the factor $\tilde{F}\left(\frac{k}{z_1}(\mathbf{x}' + \mathbf{x}'')\right)$ will no longer be a delta function, so that the aberration cancellation will become only approximate.

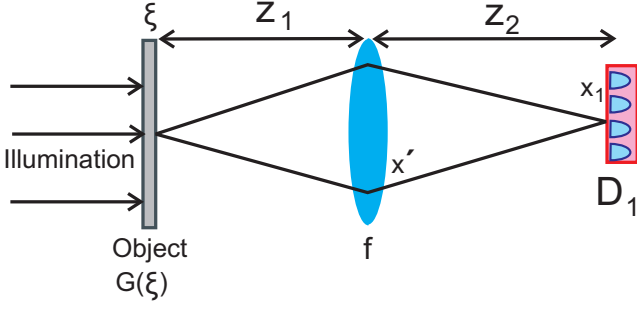


FIG. 5: (Color online) Simple incoherent imaging system. The distances z_1 and z_2 obey the imaging condition $\frac{1}{z_1} + \frac{1}{z_2} = \frac{1}{f}$.

The coincidence rate may be compared directly to the image intensity $I(x_1)$ collected by an incoherently-illuminated single-lens imaging system such as that of fig. 5. Up to overall normalization, the output intensity of the system in fig. 5, taking lens aberrations into account, is

$$I(\mathbf{x}_1) = \int d^2\xi |G(\xi)E_p(\xi)|^2 \times \left| \int d^2x' e^{-ik\mathbf{x}' \cdot ((\xi/z_1) + (\mathbf{x}_1/z_2))} e^{i\phi(\mathbf{x}')} \right|^2 = \int d^2\xi \left| G(\xi)E_p(\xi)\tilde{\Phi}\left(k\left(\frac{\xi}{z_1} + \frac{\mathbf{x}_1}{z_2}\right)\right) \right|^2, \quad (19)$$

where

$$\Phi(\mathbf{x}) = e^{i\phi(\mathbf{x})}. \quad (21)$$

Setting $E_p(\xi) = \text{constant}$ (plane wave illumination), we see that in the aberration-free case ($\phi(\mathbf{x}_1) = 0$) both $\tilde{\Phi}$ and $\tilde{\Phi}_{\text{even}}$ become delta functions, so that eqs. 17 and 20 both lead to images of the form $|G(M\mathbf{x}_1)|^2$, where $M = +1$ for eq. 17 and $M = -\left(\frac{z_2}{z_1}\right)$ for eq. 20.

The advantage of the proposed setup is clear in the case where the aberrations are all of odd order: in this case, the factor of $\tilde{\Phi}$ in eq. 20 distorts the image, whereas the image formed via eq. 17 is unaffected. However, the price to be paid for this is seen by considering the case where the aberrations are entirely even order: the factor of 2 in the exponent of eq. 15 doubles the effect of the even-order aberrations (compare equation (15) to eq. (21)). The reason for this is clear: both the signal and the idler contribute to the image and both gain extra phases from the aberration. For the odd-order terms, the two phases cancel, while in the even-order terms the phases add constructively. So, while the setup proposed here eliminates odd-order aberrations, it does so at the expense of worsening even-order aberrations. This method will therefore be of maximal benefit when the aberration term of greatest importance is of odd order and is much larger than any of the even order terms.

A further advantage is the improvement in sensitivity over standard single-detector imaging due to reduced effects of noise. For example, we can look at the effects of the detector dark current on the coincidence rate. We assume (i) that all fluctuations have zero mean, and (ii) the dark current fluctuations in one detector are uncorrelated with the signal and dark currents in the other detector. Then we can write the total detected current as the sum of the signal and dark currents (I_s and I_d), and (because of assumption (i)) further split each signal and dark current into mean and fluctuation parts:

$$I_j = I_{sj} + I_{dj} = \langle I_{sj} \rangle + \langle I_{dj} \rangle + \delta I_{sj} + \delta I_{dj}, \quad (22)$$

where $j = 1, 2$ labels the detector. If the average background counting rate is subtracted off, the remaining coincidence rate is proportional to the correlation function between the measured currents in the two detectors,

$$G^{(2)}(I_1, I_2) = \langle I_1 I_2 \rangle - \langle I_1 \rangle \langle I_2 \rangle. \quad (23)$$

Substituting eq. 22 into eq. 23 and making use of the two assumptions above, a few lines of algebra quickly shows that the effect of the dark current completely cancels out of the correlation function.

The effect of quantum noise is more complicated, and has been studied recently in a number of papers [22–25]. Since the effect of quantum noise is strongly dependent on the parameters of the experiment, it is hard to draw general conclusions about its relative effect on quantum versus classical imaging. In some cases quantum imaging offers benefits on this front as well, but the situation has to be examined on a case by case basis. See the references cited above for more detail.

IV. ABERRATION-CANCELLATION WITH A CLASSICAL SOURCE

The odd-order aberration cancellation effect in the previous section occurs because the beams strike the lens in a spatially anticorrelated manner, leading to the structure $\phi(\mathbf{x}') + \phi(\mathbf{x}'') = \phi(\mathbf{x}') + \phi(-\mathbf{x}')$ in the exponents. The entanglement of the beams plays no role here. The same effect may be produced by any method that requires light to strike diametrically opposite points on the lens simultaneously.

To illustrate this, we display in fig. 6 an apparatus with classical illumination that achieves the same effect. A narrow beam illuminates a rotating mirror, which reflects the beam onto a beam splitter. (The rotating mirror could be replaced by any form of beam-steering modulator.) The reflected and transmitted beams leave the beam splitter with opposite transverse momenta $\pm \mathbf{q}$, striking the lens on opposite sides of the axis. Over time, as the mirror rotates, the entire area of the lens is filled. As before, the object is placed in front of the bucket detector D_2 . The impulse response function for the full system is the product of those of the two individual beams,

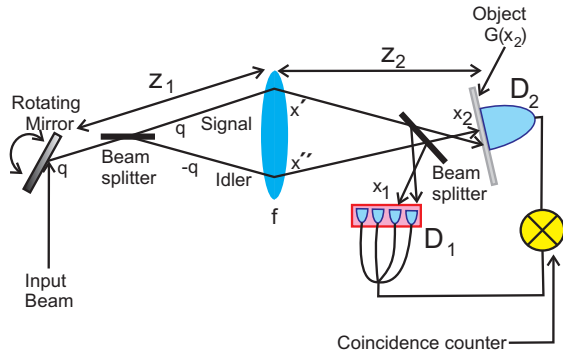


FIG. 6: (Color online) Implementation of scheme of fig. 2 using narrow classically correlated beams for illumination.

once again leading to the same $\phi(\mathbf{x}') + \phi(-\mathbf{x}')$ structure, and to odd-order aberration cancellation.

V. CONCLUSIONS

In this paper, we have shown that correlated photon methods may be used to manipulate the effects of aber-

ration in a simple optical imaging system. Specifically, the scheme described here will eliminate effects of odd-order aberrations induced by the optical system at the expense of amplifying the effects of even-order aberrations. The results here are in a sense complementary to those of [13–15], which involved cancellation of *even*-order aberrations induced by the object itself (not by the optical system) in interferometry by means of entangled photons. It remains for future investigations to see what additional types of manipulation of phase effects may be possible using variations on the methods considered here.

Acknowledgments

This work was supported by a U. S. Army Research Office (ARO) Multidisciplinary University Research Initiative (MURI) Grant; by the Defense Advanced Research Projects Agency (DARPA), and by the Bernard M. Gordon Center for Subsurface Sensing and Imaging Systems (CenSSIS), an NSF Engineering Research Center.

-
- [1] T.B. Pittman, Y.H. Shih, D.V. Strekalov, A.V. Sergienko, *Phys. Rev. A* **52** R3429 (1995).
 - [2] R.S. Bennink, S.J. Bentley, R.W. Boyd, *Phys. Rev. Lett.* **89**, 113601 (2002)
 - [3] R.S. Bennink, S.J. Bentley, R.W. Boyd, J.C. Howell, *Phys. Rev. Lett.* **92**, 033601 (2004)
 - [4] A. Gatti, E. Brambilla, M. Bache, L.A. Lugiato, *Phys. Rev. A* **70**, 013802 (2004).
 - [5] Y.J. Cai, S.Y. Zhu, *Phys. Rev. E* **71**, 056607 (2005).
 - [6] A. Valencia, G. Scarcelli, M. D'Angelo, Y.H. Shih, *Phys. Rev. Lett.* **94**, 063601 (2005).
 - [7] G. Scarcelli, V. Berardi, Y.H. Shih, *Phys. Rev. Lett.* **96**, 063602 (2006).
 - [8] F. Ferri, D. Magatti, A. Gatti, M. Bache, E. Brambilla, L.A. Lugiato, *Phys. Rev. Lett.* **94**, 183602 (2005)
 - [9] D. Zhang, *Opt. Lett.*, **30**, 2354 (2005).
 - [10] J.D. Franson, *Phys. Rev. A* **45** 3126 (1992).
 - [11] A.M. Steinberg, P.G. Kwiat, R.Y. Chiao, *Phys. Rev. Lett.* **68** 2421 (1992).
 - [12] O. Minaeva, C. Bonato, B.E.A. Saleh, D.S. Simon, A.V. Sergienko, *Phys. Rev. Lett.* **102** 100504 (2009).
 - [13] C. Bonato, A.V. Sergienko, B.E.A. Saleh, S. Bonora, P. Villorresi, *Phys. Rev. Lett.* **101** 233603 (2008).
 - [14] C. Bonato, D.S. Simon, P. Villorresi, A.V. Sergienko, *Phys. Rev. A* **79** 062304 (2009).
 - [15] D.S. Simon, A.V. Sergienko, *Phys. Rev. A* **80**, 053813 (2009).
 - [16] M. Born and E. Wolf, *Principles of Optics*, 7th ed., Cambridge University Press, New York (1999).
 - [17] H.A. Buchdahl, *Optical Aberration Coefficients*, Dover Publications (1968).
 - [18] J.C. Wyant and K. Creath, *Basic Wavefront Aberration Theory for Optical Metrology*, in *Applied Optics and Optical Engineering*, Vol. XI, Academic Press (1992).
 - [19] D.N. Klyshko, *Zh. Eksp. Teor. Fiz.* **83**, 1313 (1982) [Soviet JETP **56** 753 (1982)].
 - [20] D.N. Klyshko, *Zh. Eksp. Teor. Fiz.* **94**, 82 (1988) [Soviet JETP **67** 1131 (1988)].
 - [21] A.F. Abouraddy, B.A. Saleh, A.V. Sergienko, M.C. Teich, *J. Opt. Soc. Am. B* **19**, 1174 (2002).
 - [22] J. Cheng and S.S. Han, *Chin. Phys. Lett.* **22**, 1676 (2004).
 - [23] A. Gatti, M. Bache, D. Magatti, E. Brambilla, F. Ferri, L.A. Lugiato *J. Mod. Opt.* **53** 739 (2006).
 - [24] B.E.A. Saleh, M.C. Teich, in A.T. Friberg and R. Dändliker, eds., *Advances in Information Optics and Photonics*, **PM183** (SPIE Press, Bellingham, WA 2008), Chapter 21.
 - [25] B.I. Erkmen and J.H. Shapiro, *Phys. Rev. A* **79**, 023833 (2009).